Synthesis of Poly(butyl methacrylate) in Three-Component Cationic Microemulsions

J. I. ESCALANTE,[1] L. A. RODRÍGUEZ-GUADARRAMA,[1] E. MENDIZÁBAL,[1] J. E. PUIG,[1,*] R. G. LÓPEZ,[2] and I. KATIME[3]

[1]Departamento de Ingeniería Química, Universidad de Guadalajara, Boul. M. García Barragán #1451, Guadalajara, Jalisco 44430, Mexico; [2]Centro de Investigaciones en Química Aplicada, Saltillo, Coahuila 25100, Mexico; [3]Departamento de Química Física, Facultad de Ciencias, Universidad del País Vasco, Bilbao, Spain

SYNOPSIS

The polymerization of butyl methacrylate in three-component microemulsions prepared with the cationic surfactant dodecyltrimethylammonium bromide is reported here as a function of monomer and surfactant content in parent microemulsions, type and concentration of initiator, and temperature. Fast reaction rates and high conversions are achieved in all cases. Final latexes are bluish-opaque and stable, and contain spherical particles with diameters in the range of 20 to 30 nm, depending on composition of the parent microemulsions and reaction conditions. Each of these particles is composed of a few macromolecules of high molecular weight (2 to 4 $\times$ 10^6 Dalton). Both particle size and average molecular weight remain constant throughout the reaction, suggesting a continuous nucleation mechanism. Analysis of the molecular weight distribution indicates that the controlling termination mechanism is chain-transfer to monomer. © 1996 John Wiley & Sons, Inc.

INTRODUCTION

The synthesis of high-molecular-weight polymers in the form of nanoparticles dispersed in an aqueous (or organic) medium with fast reaction rates can be easily achieved by microemulsion polymerization.[1-4] Since the first report in 1980,[5] many papers on polymerization in direct, inverse, and bicontinuous microemulsions have appeared.[6-22] Atik and Thomas reported the polymerization of styrene in aqueous cetyl trimethyl ammonium bromide (CTAB) micellar solutions,[6] but these solutions were too diluted to be considered truly microemulsion phases. The first polymerization in three-component (i.e., surfactant, water, and styrene) one-phase microemulsions was reported by our group in 1990.[8] After that, several reports on the polymerization of various monomers in ternary o/w microemulsions have appeared.[16-21] Polymerization in three-component microemulsions is easier to model and to understand because, among other factors, partitioning of components between the microemulsion domains is simpler to measure or to estimate, and no extraneous chain-transfer agent or modifiers (such as alcohol cosurfactants or electrolytes) are present. Also, studying polymerization in three-component microemulsions is useful in understanding the effects on kinetics of adding alcohol, electrolytes, or other ingredients.

The kinetics and mechanism of microemulsion polymerization depend strongly on monomer solubility in water. For instance, both molecular weight and particle size remain constant throughout the polymerization of the water-insoluble styrene,[22] whereas both particle size and molecular weight increase with reaction time during the polymerization of the more water-soluble tetrahydrofurfuryl methacrylate.[17] Hence it is important to examine systematically the role of monomer solubility in this kind of polymerization process.

Here we report on the polymerization of butyl methacrylate (BuMA), which is a monomer with low solubility in water,[23] in ternary microemulsions prepared with the cationic surfactant dodecyltrimethylammonium bromide (DTAB), as a function of temperature, BuMA and DTAB concentrations, and

* To whom correspondence should be addressed.

Journal of Applied Polymer Science, Vol. 62, 1313–1323 (1996)
 CCC 0021-8995/96/091313-11

type and concentration of initiator. Here we show that stable, bluish-to-opaque latexes containing poly(BuMA) particles with sizes around 20 to 30 nm and molecular weights of several millions can be produced with fast reaction rates by this method.

EXPERIMENTAL

Reagent grade BuMA from Scientific Polymer Products (Ontario, NY) was distilled in vacuum before used. DTAB (99% pure from Tokyo Kasei) was recrystallized from an ethanol/ethyl ether mixture (50 : 50 vol/vol). Potassium persulfate ($K_2S_2O_8$ or KPS) and hydroquinone were reagent grade from Aldrich (Milwaukee, WI). 2,2′-Azobis (2-amidinopropane) hydrochloride (V-50) from Wako (Osaka, Japan) was recrystallized from methanol. HPLC-grade tetrahydrofurane (Merck, Rahway, NJ) was used as the mobile phase in gel permeation chromatography (GPC).

The one-phase microemulsion regions at 25 and 60°C were determined visually by titrating aqueous DTAB micellar solutions with BuMA. The phase diagram at 60°C was determined with monomer containing 100 ppm of methyl ester hydroquinone to inhibit thermal polymerization. One-phase samples were examined through cross-polarizers to determine if they were birefringent. Only non-birefringent, one-phase samples were considered microemulsions. Microemulsion conductivities were measured at 1000 Hz with an Orion 101 conductimeter and a Yellow Spring Instrument immersion cell (cell constant equal to 1.12 cm^{-1}). The cell was calibrated with KCl aqueous solutions of known conductivities.[24]

Polymerization was carried out at 45, 50, 55, or 60°C in a 100-mL glass reactor. The reactor was loaded with microemulsion, heated to the reaction temperature, and sparged with argon for 30 min before a small amount of a concentrated aqueous solution of KPS or V-50 was injected. The reacting system was continuously stirred and sparged with argon throughout the reaction. Polymer was isolated by filtration after precipitation with methanol, washed with hot water, and dissolved in THF for GPC analysis.

Quasielastic light scattering (QLS) measurements were made with a Malvern 4700 QLS apparatus equipped with a He–Ne ion laser (λ = 644 nm). Intensity correlation data were analyzed by the method of cumulants to provide the average decay rate, $\langle \Gamma^2 \rangle$ ($=q^2D$), where $q = (4\Pi n/\lambda) \sin(\theta/2)$ is the scattering vector, n the index of refraction, D the diffusion coefficient, and the variance, ν ($=[\langle \Gamma^2 \rangle - \langle \Gamma \rangle^2]/\langle \Gamma \rangle^2$), which is a measure of the width of the distribution of the decay rate. The measured diffusion coefficients were represented in terms of apparent radii by means of Stokes law, assuming that the solvent has the viscosity of water. Latexes were diluted up to 100 times and filtered through 0.2 μm Millipore filters before QLS measurements to minimize particle–particle interactions and to remove dust particles.

Average molecular weights and molecular weight distributions (MWD) were measured with a Perkin Elmer LC 30 size exclusion chromatograph equipped with a LC30 refractive index detector and Dawn multiangle light scattering detector from Wyatt Technology (Santa Barbara, CA).

RESULTS

Partial phase diagrams of mixtures of DTAB, water, and BuMA at 25 and 60°C are shown in Figure 1. One-phase microemulsions form at the H_2O–DTAB side of the ternary phase diagram. The extension of the one-phase region increases with temperature. Microemulsions are transparent and fluid except at high surfactant concentrations where samples are transparent (and nonbirefringent when examined through cross-polarizers) but highly viscous. Upper phase boundaries (indicated by dashed lines in Fig. 1) were not determined exactly because of the high viscosity of the samples. Conductivity is high and increases with surfactant concentration and with temperature (Fig. 2). As expected, conductivity de-

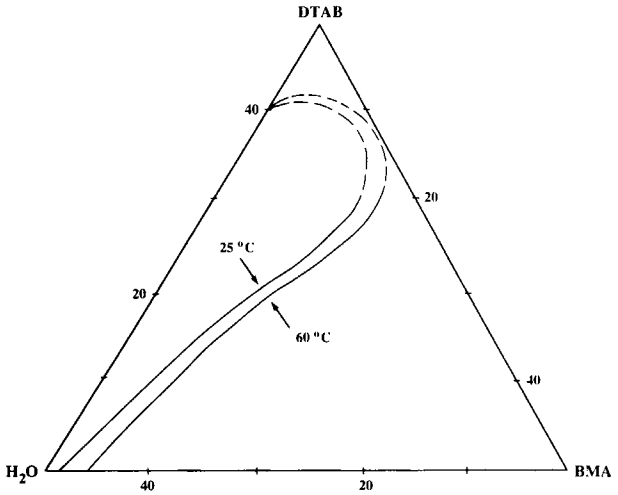

Figure 1 Extent of the one-phase region in a partial phase diagram of DTAB/BuMA/water at 25 and 60°C. The upper phase boundaries (indicated with dashed lines) were not determined exactly.

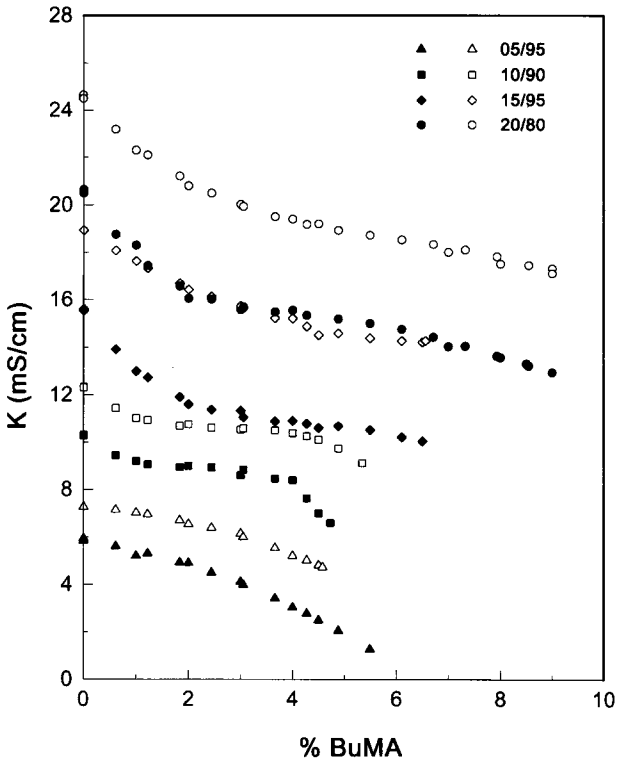

Figure 2 Electrical conductivity (κ) of DTAB/BuMA/water microemulsions at 25°C (solid symbols) and 60°C (open symbols) at various DTAB/water weight ratios.

creases upon BuMA addition, probably because of micelle growth.

Conversion versus time as a function of BuMA concentration in the parent microemulsions prepared at a constant DTAB/H_2O weight ratio of 15/85 (wt/wt) are shown in Figure 3. Polymerization was initiated with 1% V-50 at 60°C—here, initiator concentrations are given in wt % with respect to initial monomer concentration. Polymerization is fast (near 100% conversion in 10 min) and the transparent microemulsions take on a light blue tinge at the onset of reaction and become increasingly turbid as the reaction proceeds. Initial reaction rates depend slightly on initial BuMA concentration. Only two rate intervals are observed here (inset in Fig. 3): one where the polymerization rate increases rapidly, followed by a decreasing rate interval. This behavior is typical for the microemulsion polymerization of water-insoluble monomers.[4] The maximum reaction rate, which occurs at about 30% conversion, increases with BuMA concentration to an exponent of 0.4. Dependence of polymerization rate on monomer concentration has also been reported in other reacting microemulsions.[8,9,19] The appearance of final latexes ranges from bluish to opaque depending on the BuMA concentration. Also, the turbidity increases with initial BuMA content in the parent microemulsions.

Figure 4 shows conversion curves for the polymerization of microemulsions containing 6 wt % BuMA and different DTAB/H_2O weight ratios initiated with 1% V-50, which is a water-soluble initiator that decomposes into two cationic free radicals. The polymerization rate is fast and increases with surfactant content in the parent microemulsions. Conversions near 100% are achieved in less than 15 min with the microemulsions made with 20/80 and 15/85 DTAB/water ratios. With the 10/90 sample, the reaction is much slower. Only two rate intervals are again observed here, with a maximum in reaction rate at conversions around 35% (inset in Fig. 4). This behavior is not apparent for the 10/90 microemulsion; however, by enlarging the scale (not shown), the two rate intervals are clearly observed.

Polymerization of microemulsions containing 6 wt % BuMA and a DTAB/H_2O ratio of 15/85 was studied as a function of V-50 concentration (Fig. 5). The overall reaction rate is very fast and in-

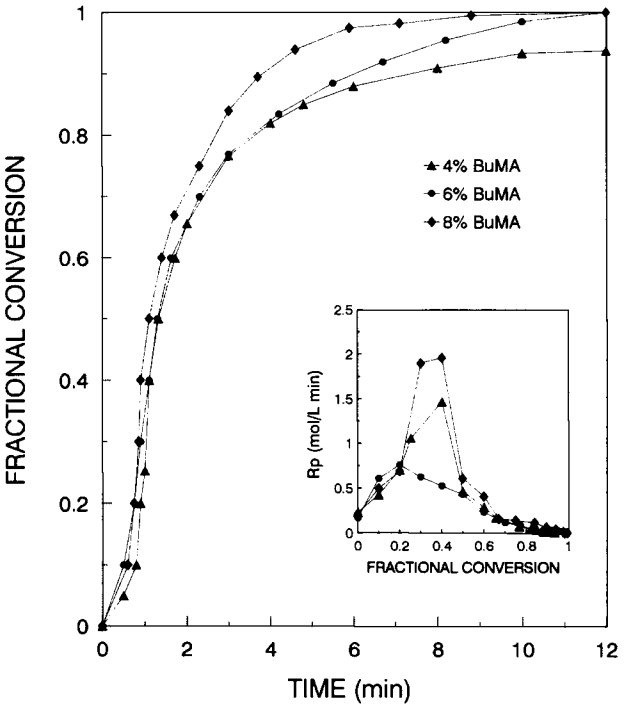

Figure 3 Conversion as a function of time for the polymerization at 60°C initiated with 1% V-50 of microemulsions prepared at a constant DTAB/water line of 15/85 containing various BuMA concentrations. Inset: polymerization rate as a function of conversion for data shown in the figure.

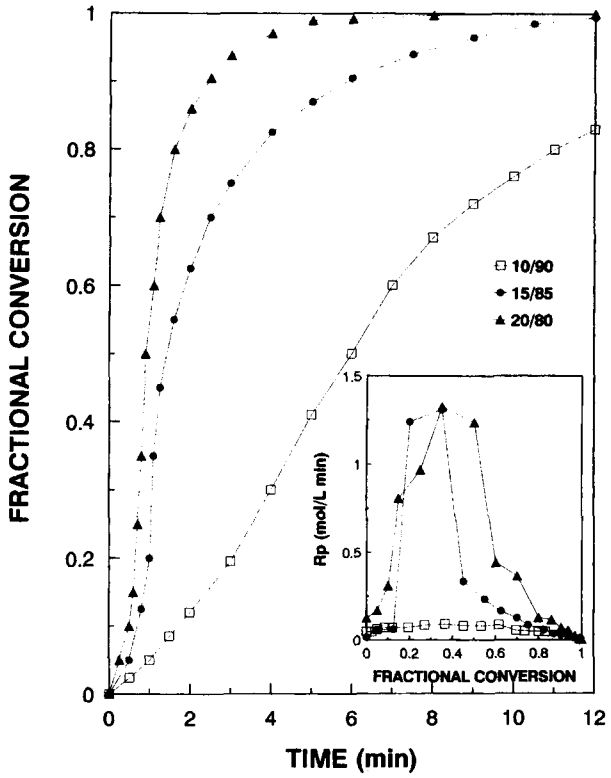

Figure 4 Conversion as a function of time for the polymerization at 60°C initiated with 1% V-50 of microemulsions prepared with 6 wt % BuMA and different DTAB/water weight ratios. Inset: polymerization rate as a function of conversion for data shown in the figure.

creases with initiator concentration. There is no induction time at any V-50 concentration. Final conversion (after 12 min of reaction) augments with increasing initiator concentration. The overall reaction rate does not exhibit a constant-rate interval but only increasing and decreasing rate intervals (inset in Fig. 5). Maximum polymerization rate increases with V-50 concentration with an exponent of 0.95.

The effect of temperature on the polymerization of 6 wt % BuMA microemulsion initiated with 1% V-50 is shown in Figure 6. As expected, reaction rate and conversion increase with increasing temperature as a consequence of the increment in the flux of free radicals and in the propagation rate constant. The maximum polymerization rate follows an Arrhenius dependence with temperature. From the slope of plots of log $R_{p_{max}}$ versus T^{-1}, an activation energy of 31.4 Kcal/mol was obtained (inset in Fig. 6).

Similar experiments were performed with KPS, which is a water-soluble initiator that decomposes into anionic free radicals. Conversion curves as a function of KPS concentration for the polymerization of 6 wt % BuMA microemulsions are shown in Figure 7. Reaction rates and final conversions increase as the amount of KPS increases, although the reactions are slower than those initiated with V-50 (Figs. 5 and 7). Again, only two rate intervals are detected (inset in Fig. 7). The maximum polymerization rate increases as $[KPS]^{1.5}$.

The effect of temperature on the polymerization of a 6 wt % BuMA microemulsion made with 15/85 DTAB/H_2O is reported in Figure 8. Again, reaction rates and final conversions increase with increasing temperature. The maximum polymerization rate also follows an Arrhenius behavior with temperature with an activation energy of 35.4 Kcal/mol (inset in Fig. 8). Notice that the reaction rate slows substantially for temperatures below 55°C because the decomposition rate of KPS decays rapidly in this temperature range.[23]

Particle size and molecular weight were followed as a function of conversion for the polymerization of 6 wt % BuMA in a 15/85 DTAB/H_2O microemulsion initiated with 1% V-50 at 60°C. Results

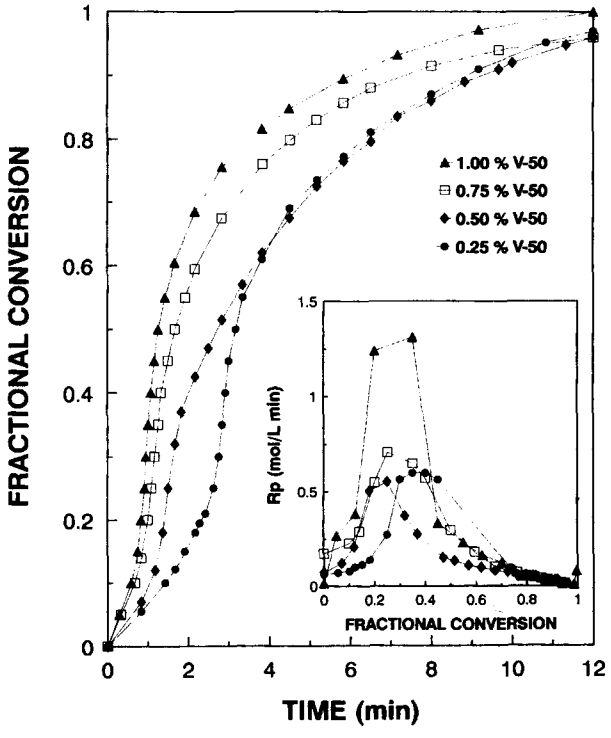

Figure 5 Conversion as a function of time for the polymerization at 60°C initiated with different V-50 concentrations of microemulsions containing 6 wt % BuMA and a DTAB/water ratio of 15/85. Inset: polymerization rate as a function of conversion for data shown in the figure.

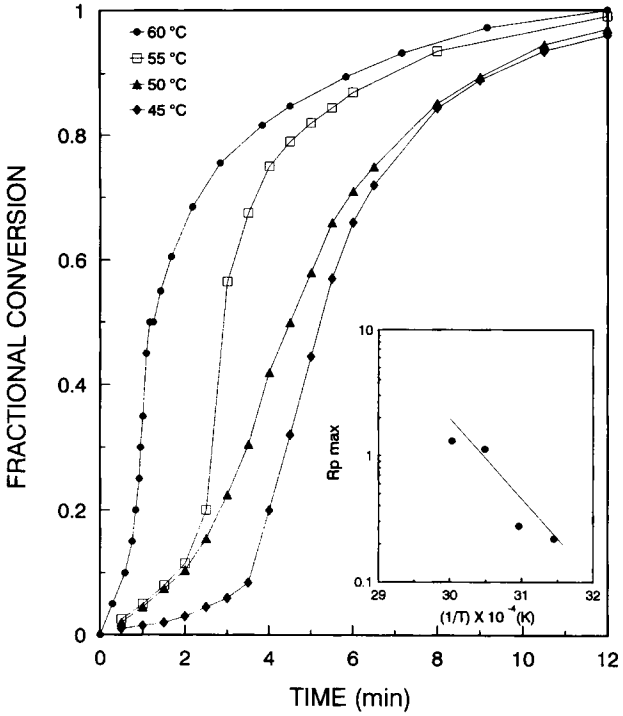

Figure 6 Conversion as a function of time for the polymerization initiated with 1% V-50 at different temperatures for microemulsions containing 6 wt % BuMA and a DTAB/water ratio of 15/85. Inset: Arrhenius plot of $R_{p_{max}}$ versus T^{-1}.

in Figure 9 show that both particle size and average molecular weight remain constant throughout the reaction—polymer samples below 10% conversion could not be isolated due to the small amounts of polymer formed early in the reaction. The number of polymer chains per particle, estimated by assuming that the density of the particles is that of bulk poly(BuMA), is between 2 and 4 (Tables I–III). This type of behavior appears to be typical of polymerization of water-insoluble monomers in microemulsion media.[22] The characteristics of the latexes at the end of the different reactions studied here are compiled in Tables I through III.

The effects of initial monomer concentration, type and concentration of initiator, and temperature on final average particle size and weight-average molecular weight are shown in Figure 10. Particle size increases with BuMA concentration as $D_p \propto [\text{BuMA}]^{0.12}$ [Fig. 10(a)]. Particle size is independent of initiator type but it decreases with initiator concentration to an exponent of −0.08 for V-50 and −0.05 for KPS [Fig. 10(b)]. Molecular weight decreases with initiator concentration with an exponent of −0.15 for V-50 and −0.17 for KPS [Fig. 10(b)]. Particle size decreases as reaction temperature increases, with both KPS and V-50. We found that $D_p \propto T^{-0.79}$ for V-50 and $D_p \propto T^{-0.94}$ for KPS [Fig. 10(c)]. The molecular weight also decreases with increasing temperature [Fig. 10(c)].

In polymerization reactions the MWD is controlled mainly by chain-stopping events.[25] In a zero-one free radical system, all chain-stopping events are caused by entry of radicals—which produces instantaneous combination—and transfer to monomer, polymer, or a chain transfer agent. For this case, the instantanteous MWD is given by

$$P(M) = \exp\left(-\frac{(C_M k_{tr,M} + [A]k_{tr,A} + \rho)M}{k_P C_M M_0}\right) \quad (1)$$

where C_M is the monomer concentration *in* the particle; $k_{tr,M}$ is the rate constant of chain transfer to monomer; $[A]$ is the concentration of chain-transfer agent species; $k_{tr,A}$ is the rate constant of chain transfer to species A; ρ is the generation rate of free radicals; k_P is the propagation rate constant; and M_0 is the molecular weight of the monomer.[25]

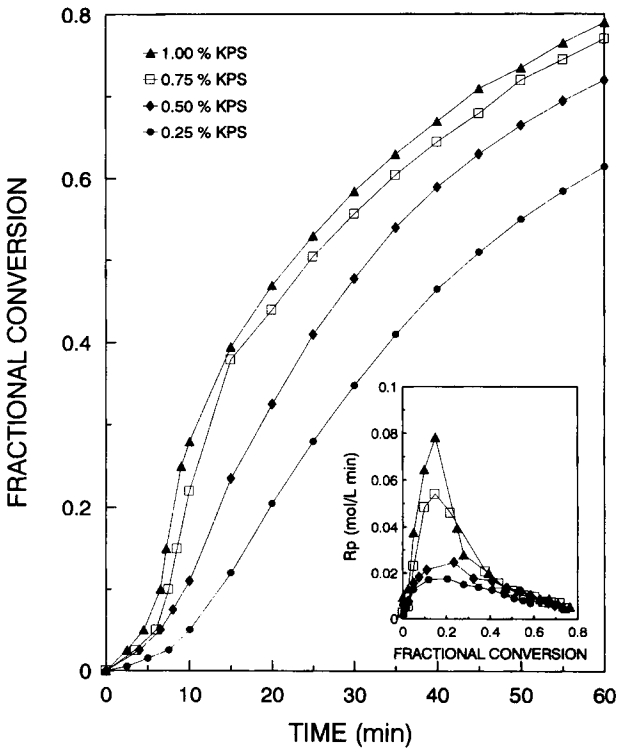

Figure 7 Conversion as a function of time for the polymerization at 60°C initiated with different KPS concentrations for microemulsions containing 6 wt % BuMA and a DTAB/water ratio of 15/85. Inset: polymerization rate as a function of conversion for data shown in the figure.

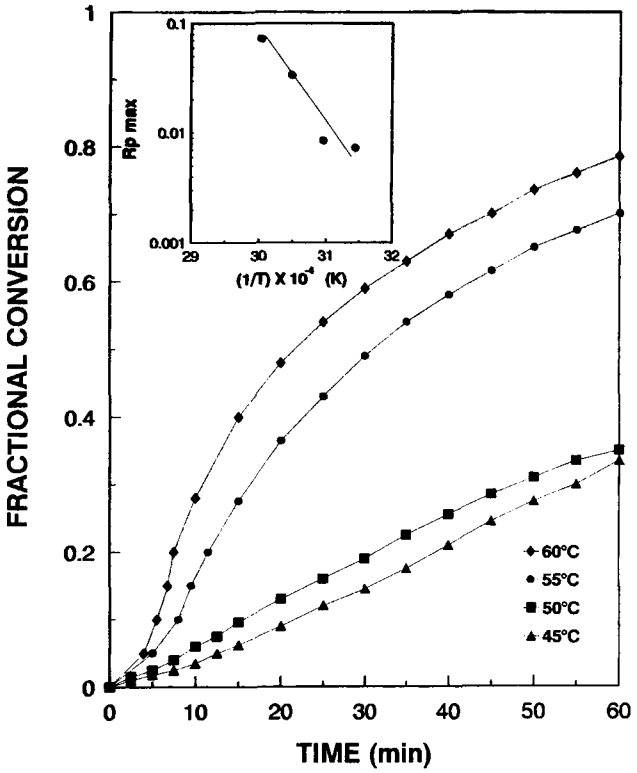

Figure 8 Conversion as a function of time for the polymerization initiated with 1% KPS at different temperatures for microemulsions containing 6 wt % BuMA and a DTAB/water ratio of 15/85. Inset: Arrhenius plot of $R_{p_{max}}$ versus T^{-1}.

However, if: (1) there is no chain transfer agent present, (2) all chain transfer is only to monomer (not to polymer), and (3) $\rho \ll k_{tr,M}C_M$, which is typical in zero-one free radical emulsion or microemulsion polymerization,[19,22,25] then

$$P(M) = \exp\left(-\frac{k_{tr,M}M}{k_P M_0}\right) \qquad (2)$$

Hence the best way to obtain information about the controlling termination mechanism is to plot the log of $P(M)$ against M. Figure 11 shows plots of log $P(M)$ versus M for the polymerization of 6% BuMA in 15/85 DTAB/H_2O microemulsions as a function of conversion. Plots are linear and parallel at all conversions, in agreement with eq. (2), except at the low end of the MWD, suggesting that chain-transfer to monomer is the dominant mechanism under these conditions. From the slope of these plots, a value of $k_{tr,M}/k_P$ of 6.5 ($\pm$1) $\times 10^{-5}$ was estimated, which is close to the value reported in the literature (1.5×10^{-5}).[23]

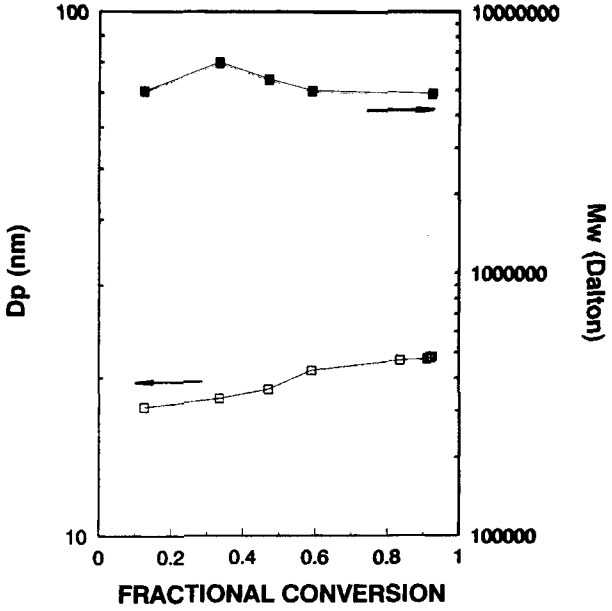

Figure 9 Particle size (D_p) and weight-average molecular weight (M_w) as a function of conversion for the polymerization at 60°C initiated with 1% V-50 of a microemulsion containing 6 wt % BuMA and a DTAB/water ratio of 15/85. Error bars are smaller than size of symbols.

Plots of log $P(M)$ versus M for the final products of the polymerization of BuMA using different amounts of V-50 are shown in Figure 12. Again, plots are linear and they have similar slopes. The value of $k_{tr,M}/k_P$, calculated from these plots, is 7.5 ($\pm$0.5) $\times 10^{-5}$. In all the cases examined here plots are linear, indicating that chain-transfer to monomer is the main termination mechanism. Table IV summarizes the values of $k_{tr,M}/k_P$ calculated from the plots of log $P(M)$ versus M for the different polymerization reactions carried out in this work.

Table I Particle Size (D_p), Weight-Average Molecular Weight (M_w), Polydispersity (M_w/M_n), and Average Number of Polymer Chains per Particle (n_c) of the Final Latexes Produced by the Polymerization of BuMA Microemulsions

% BuMA	D_p (nm)	$M_w \times 10^{-6}$ (DALTON)	M_w/M_n	n_c
4	19.9	3.2	1.22	1.2
6	20.8	3.3	1.26	1.3
8	21.6	3.2	1.11	1.1

Prepared at a DTAB/water weight ratio of 15/85 and different BuMA concentrations initiated at 60°C with 1% V-50 (with respect to monomer).

Table II Particle Size (D_p), Weight-Average Molecular Weight (M_w), Polydispersity (M_w/M_n), and Average Number of Polymer Chains per Particle (n_c) of the Final Latexes Produced by the Polymerization of 6 Wt % BuMA Microemulsions

C_I	D_p (nm)	$M_w \times 10^{-6}$ (DALTON)	M_w/M_n	n_c
0.25% V-50	22.2	4.2	1.33	1.3
0.50% V-50	21.8	4.00	1.16	1.1
1.00% V-50	20.8	3.3	1.26	1.3
0.25% KPS	24.1	2.6	1.28	2.5
0.50% KPS	22.8	2.34	1.64	3.0
1.00% KPS	21.6	2.1	1.24	2.1

Prepared at a DTAB/water weight ratio of 15/85 initiated at 60°C with different concentrations of V-50 or KPS.

DISCUSSION AND CONCLUSIONS

Transparent one-phase microemulsions of BuMA, water, and DTAB were found at 25 and 60°C at the water-rich corner of the phase diagram (Fig. 1). The uniphasic region increases with temperature. The extent of the microemulsion region at 25 and 60°C is similar to that reported for the DTAB/water/methyl methacrylate (MMA) system[19] and larger than that for the DTAB/water/styrene system.[8] This is probably because of the more amphiphilic character of BuMA (and MMA) which allows them to behave as cosurfactants. Unpolymerized microemulsions are optically transparent and have low viscosities (<10 cP) for DTAB concentrations smaller than 20 wt %. Concentrated microemulsions

Table III Particle Size (D_p), Weight-Average Molecular Weight (M_w), Polydispersity (M_w/M_n), and Average Number of Polymer Chains per Particle (n_c) of the Final Latexes Produced by the Polymerization of 6 Wt % BuMA Microemulsions

Temp. (°C)	D_p (nm)	$M_w \times 10^{-6}$ (DALTON)	M_w/M_n	n_c
		1.00% V-50		
45	27.3	3.8	1.10	2.1
60	20.8	3.3	1.26	1.3
		1.00% KPS		
45	29.8	4.8	1.53	3.0
60	21.6	2.1	1.24	2.1

Prepared at a DTAB/water weight ratio of 15/85 initiated at 45°C or 60°C with 1% V-50 or KPS.

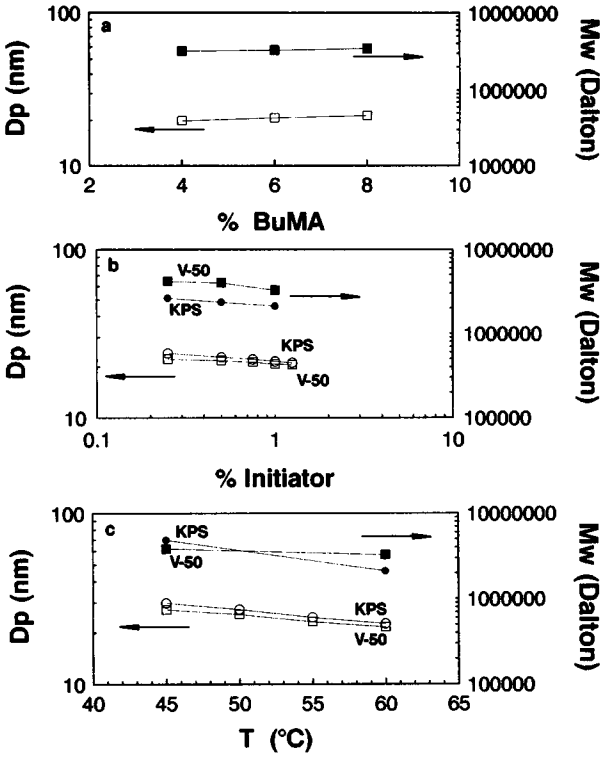

Figure 10 (a) Particle size (D_p) and weight-average molecular weight (M_w) in final latexes as a function of BuMA content in parent microemulsions prepared at a constant DTAB/water ratio of 15/85 weight ratio and polymerized with 1% V-50. (b) Particle size (D_p) and weight-average molecular weight (M_w) in final latexes as a function of initiator concentration for the polymerization of a 6 wt % BuMA microemulsion prepared at a 15/85 DTAB/water weight ratio. (c) Particle size (D_p) and weight-average molecular weight (M_w) as a function of temperature for the polymerization of a 6 wt % BuMA microemulsion prepared at a 15/85 DTAB/water weight ratio.

are also transparent but highly viscous, and their viscosity increases with increasing surfactant content.

Electrical conductivity of these microemulsions is high, suggesting a water-continuous microstructure. The decrease in microemulsion conductivity upon increasing BuMA content suggests micellar growth (Fig. 2). QLS and small-angle neutron scattering (SANS) experiments on styrene/DTAB/D_2O microemulsions indicate that these microemulsions contain oil droplets (swollen micelles) dispersed in an aqueous phase saturated with monomer and surfactant.[22] Since BuMA is also a water-insoluble, nonpolar monomer, it is likely that the microstructure of the BuMA microemulsions is the same than that of the styrene/DTAB/water microemulsions.

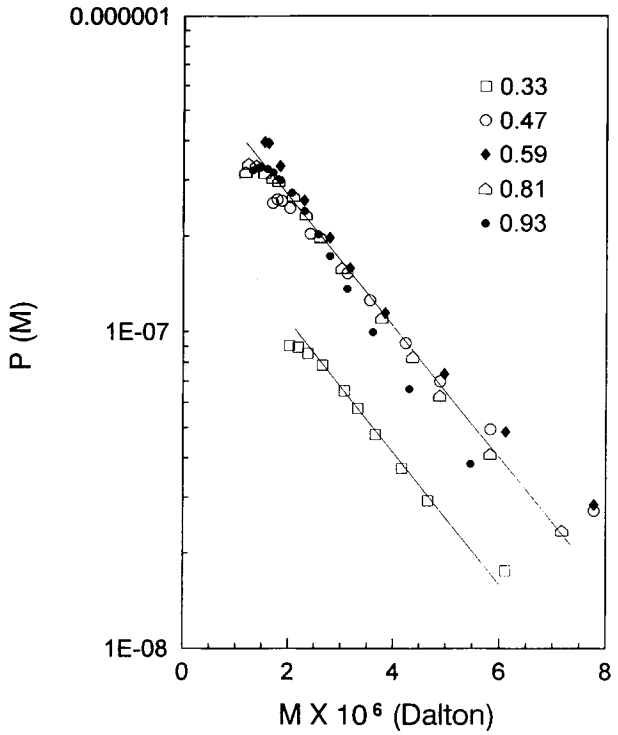

Figure 11 Logarithm of the instantaneous number MWD, $P(M)$, versus molecular weight, M, as a function of fractional conversion for the polymerization of a 6 wt % BuMA microemulsion prepared at a 15/85 DTAB/water weight ratio initiated with 1% V-50 at 60°C.

Polymerization of BuMA in DTAB microemulsions is very rapid (Figs. 3–8) and faster than those reported for styrene and for MMA in DTAB microemulsions.[8,19] The reaction with BuMA is faster than that of styrene in microemulsions with similar compositions because the propagation rate constant for BuMA (k_P = 0.47 m^3/mol · s at 60°C)[23] is higher than that of styrene [k_P = 0.19 m^3/(mol s) at 60°C).[23] On the other hand, the propagation rate constant for MMA (k_P = 0.513 m^3/(mol s) at 60°C)[23] is similar to that for BuMA. Nevertheless, the concentration of DTAB in the MMA microemulsions reported elsewhere[19] is smaller (7 wt %) than the ones studied here. This may explain why the reaction rate in BuMA microemulsions is faster than that in MMA microemulsions, since it is known that the polymerization rate in microemulsion media increases with surfactant content (see Fig. 4, Pérez-Luna and coworkers,[8] and Rodríguez-Guadarrama and colleagues[19]).

The transparent microemulsions become increasingly turbid as the reaction proceeds because of particle growth and the increase in the refractive index difference between the particles and the suspending medium. Final latexes range from bluish-transparent to opaque, depending on BuMA and surfactant content in parent microemulsions and on reaction conditions. More opaque latexes are obtained by increasing the monomer content, decreasing the surfactant or initiator concentration, or decreasing the reaction temperature.

In contrast to emulsion polymerization, the microemulsion polymerization rate and final conversion depend on the initial BuMA content (Fig. 3). In emulsion polymerization, most of the monomer is in the emulsified droplets—only a small amount of the monomer is in the micelles and in the aqueous phase. These droplets do not participate in the reaction except as reservoirs of monomer.[26,27] In microemulsion polymerization, on the other hand, almost all of the monomer is in the microemulsion droplets. These droplets compete with the monomer dissolved in the aqueous phase for the capture of free radicals. In fact, it has been shown for emulsion polymerization that by reducing the size of the emulsified droplets to produce a miniemulsion, the polymerization is carried out mainly in the monomer droplets.[28] Hence, as the concentration of monomer in the parent microemulsions increases, the number

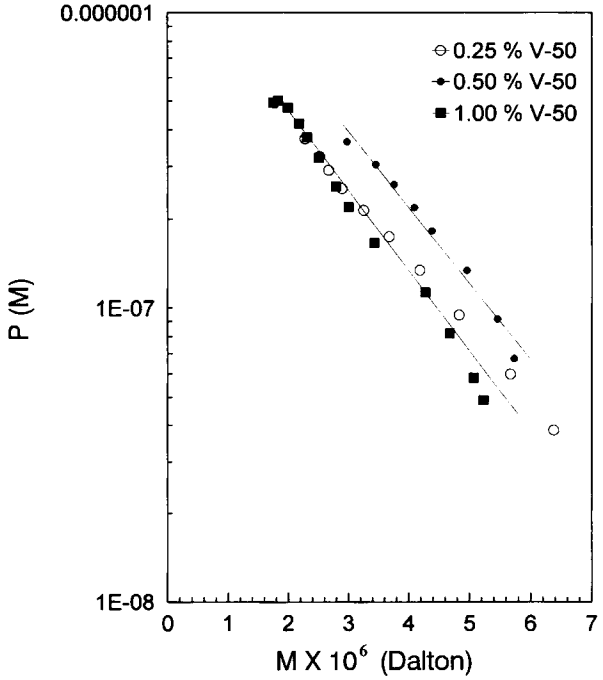

Figure 12 Logarithm of the instantaneous number MWD, $P(M)$, versus molecular weight, M, at the end of the reaction for the polymerization of a 6 wt % BuMA microemulsion prepared at a 15/85 DTAB/water weight ratio initiated with various concentrations of V-50 at 60°C.

Table IV Values of $k_{tr,M}/k_p$ for the Different Polymerizations Reported Here, Obtained from the Plots of the Logarithm of the Instantaneous Number-Average Molecular Weight Versus Molecular Weight

% I	$k_{tr,M}/k_p \times 10^{-5}$	BuMA (%)	$k_{tr,M}/k_p \times 10^{-5}$	Temp. (°C)	$k_{tr,M}/k_p \times 10^{-5}$	Conv. (%)	$k_{tr,M}/k_p \times 10^{-5}$
	KPS	4	9.99		KPS	12.50	6.04
0.25	1.28	6	7.09	45	7.83	33.40	7.05
0.50	14.60	8	2.35	60	27.00	47.10	6.57
1.00	27.00				V-50	59.10	6.81
	V-50			45	6.96	92.50	8.26
0.25	7.94			60	7.09		
0.50	7.24						
1.00	7.09						

and size of droplets increase which results in a higher probability of radical capture and, so, in faster reaction rates. Overall reaction rates and final conversions have also been shown to depend on the overall monomer concentration for MMA and styrene microemulsion polymerization.[8,19]

Reaction rates and final conversions also increase with increasing surfactant concentration (Fig. 4). The reason is that increasing surfactant concentration for a fixed concentration of monomer decreases the size of the microemulsion droplets but increases their number. As a result, the probability of capture of free radicals by microemulsion droplets increases and so does the reaction rate. Similar conclusions were reported for the polymerization of styrene in DTAB microemulsions.[8]

Increasing initiator concentration yields faster polymerization rates and higher conversions, regardless of the type of initiator employed (Figs. 5 and 7). The increasing polymerization rate with initiator concentration is a consequence of the increasing flux of free radicals, which increases the probability of radical capture by droplets (heterogeneous nucleation) or by monomer in the aqueous phase to induce formation of oligomers (homogeneous nucleation) to produce active particles. However, polymerization rates are faster and conversions are higher with V-50 than with KPS (Figs. 5 and 7). This can be explained by one—or a combination—of the following phenomena: (1) differences in values of the decomposition rate constant of V-50 and KPS, (2) electrostatic interactions between microemulsion droplets and the charged free radicals, and (3) chain-transfer reactions to counterions.

V-50 has a larger decomposition rate constant ($k_d = 3.2 \times 10^{-5}$ s^{-1} at 60°C)[29] than KPS ($k_d = 3.1 \times 10^{-6}$ s^{-1} at 60°C),[23] hence one should expect faster reaction rates with V-50 than with KPS. Also, KPS decomposes into negatively charged free radicals ($SO_4^{-\bullet}$) which are strongly bound to the positively charged DTAB microemulsion droplets. This effect, known as the "electrostatic cage effect",[30] reduces the concentration of the $SO_4^{-\bullet}$ free radicals in the aqueous phase and their efficiency to initiate the reaction. The electrostatic cage effect does not occur with V-50 because this initiator produces positively charged radicals which are repelled from the droplet surfaces. The electrostatic cage effect has also been observed for the polymerization of styrene and MMA in DTAB microemulsions.[8,19] For the polymerization of MMA and of MMA with *N*-methylolacrylamide in AOT microemulsions (whose droplets have negatively charged surfaces), KPS yields faster reaction rates and higher conversions at similar reaction temperatures because of the electrostatic interactions,[31,32] in spite of the fact that V-50 has a higher decomposition rate constant.

It is well-known that $SO_4^{-\bullet}$ free radicals can undergo transfer reactions with bromide counterions to produce neutral bromide radicals that do not initiate the reaction.[26] In fact, the rate constant for the reaction between sulfate free radicals and bromide ions ($k_{tr,Br} = 3.5 \times 10^9$ L/mol/s)[33] is higher than that between sulfate free radicals and styrene monomer ($k = 2 \times 10^9$ L/mol/s),[33] so bromide counterions quench the reaction. This type of transfer reaction does not seem to take place between the V-50 free radicals and the bromide ions.

As expected, reaction rates increase with temperature for both V-50 (Fig. 6) and KPS (Fig. 8) because the initiator decomposition rate increases rapidly with temperature.[27] Also, the propagation rate constant increases with temperature.[27] Both effects result in an increase in reaction rate and in overall conversion. Reaction rate follows an Arrhenius behavior with temperature with activation energies of 31.4 kcal/mol for V-50 and 35.4 kcal/mol for KPS. These values are similar to those re-

ported for the polymerization of MMA and of styrene in DTAB microemulsions.[8,19]

Analysis of the instantaneous MWD (Figs. 11 and 12) demonstrate that, regardless of the composition of the parent microemulsions, concentration and type of initiator or temperature of reaction, chain-transfer to monomer is the main termination mechanism. The low number of polymer chains per particle rules out termination by coagulation (Table IV). Also, the probability for the entry of a second radical in a reacting particle is quite small since the number of original droplets that become loci of reaction is rather low (<1% of the original number), at least for the polymerization of styrene in DTAB microemulsions.[22] For many emulsion and microemulsion polymerization reactions, chain-transfer reactions to monomer appears to be the controlling termination mechanism.[19,22,25]

Regardless of the type and concentration of initiator, the concentrations of BuMA and DTAB in parent microemulsions, and temperature, only two reaction rate intervals were observed: one in which the reaction rate increases monotonically and which ends at low conversions (<0.2–0.3), followed by another in which the polymerization rate decreases steadily (Figs. 3–8). Also, both particle size and average molecular weight remain constant throughout the reaction (Fig. 9) and the number of polymer chains per particle is unusually low (Tables I–III). These features appear to be characteristic of microemulsion polymerization except for the polymerization of relatively high water-soluble monomers such as tetrahydrofurfuryl methacrylate and vinyl acetate.[17,34] It has been suggested that the first rate interval corresponds to a nucleation rate interval that ends when all the droplets vanish. In the second or termination rate interval, the concentration of monomer within the particle diminishes steadily since there is no monomer available to maintain the monomer concentration constant.[11,18] However, a continuous nucleation of particles has also been proposed since there is enough surfactant to stabilize new particles as others grow.[7,15] For this reason, the combined effects of the increase in the number of particles (which should result in faster reaction rates) and the decrease in the average number of free radicals per particle and of monomer concentration per particle (which should result in a decrease in reaction rates) produces a maximum in the reaction rate at low conversions.

In microemulsion polymerization, there is a substantial number of droplets (ca. 2 to 5 $\times$ 10^{18} droplets/cm^3).[22] However, the number of monomer molecules in the aqueous phase, estimated from the solubility of BuMA in water,[23] is about 10 to 50 $\times$ 10^{18} molecules/cm^3, depending on temperature. Hence, at the beginning of reaction, free radicals can react either with microemulsion droplets (micellar nucleation) or with monomer in the aqueous phase. When the primary free radicals react with monomer in the aqueous phase, they grow to form oligomeric radicals which become hydrophobic enough to precipitate and yield reacting particles which can then be stabilized by excess surfactant (homogeneous nucleation), or to penetrate into a droplet to continue the reaction there. However, at the early stages of reaction, most of the surfactant is engaged in stabilizing microemulsion droplets, so the homogeneous nucleation mechanism is unlikely. However, when the microemulsion droplets disappear (at around 20% conversion), the probability of homogeneous nucleation is higher. Moreover, as particles grow, there is excess surfactant which can stabilize growing particles in the aqueous phase. The observation that average particle size and average molecular weight remain constant throughout the reaction (Fig. 9) strongly support the continuous nucleation mechanism.

Our hypothesis is that at the beginning of the reaction, initiation occurs mainly in the microemulsion droplets either by primary free radicals produced by the decomposition of the initiator, or by oligomeric radicals. However, once the microemulsion droplets disappear there is an excess of surfactant because of particle growth, which can stabilize new particles that can be produced by homogeneous nucleation in the aqueous phase or by micellar nucleation. Modeling of polymerization of styrene in three-component microemulsions made with DTAB showed that micellar nucleation at early stages of reaction followed by homogeneous nucleation better mimics experimental data.[35] Also, Full and colleagues,[22] demonstrated by SANS and QLS that the monodisperse parent microemulsions evolves into a bimodal dispersion of polymer particles and micelles. Since the probability of capturing a radical by the reacting particles is extremely low and there is monomer available to maintain the reaction, chain-transfer to monomer controls the growth of the particles.

In conclusion, we have shown that high molecular weight poly(BuMA) particles with diameters ranging between 20 and 30 nm can be produced with extremely fast reaction rates (100% conversion in less than 15 min) by microemulsion polymerization. The evidence presented here indicates that the continuous nucleation of particles and chain-transfer reactions to monomer control the kinetics of micro-

emulsion polymerization. However, a more thorough and systematic study of the role of monomer solubility in microemulsion polymerization is needed to understand the differences in kinetic behavior between water-insoluble and more water-soluble monomers.

This work was supported by CONACYT (Grant #3312-A-94) and by the European Community (Contract #CI1-CT94-0123).

REFERENCES

1. F. Candau, in *Encyclopedia of Polymer Science,* Vol. 9, H. F. Marks, N. M. Bikales, C. G. Overberger, and G. Menges, Eds., Wiley, New York, 1987, p. 718.
2. A. S. Dunn, in *Comprehensive Polymer Science,* Vol. 4, G. C. Eastwood, A. Ledwith, and P. Sigwalt, Eds., Pergamon Press, New York, 1988, p. 219.
3. F. Candau, in *Comprehensive Polymer Science,* Vol. 4, G. C. Eastwood, A. Ledwith, and P. Sigwalt, Eds., Pergamon Press, New York, 1988, p. 225.
4. J. E. Puig, in *Encyclopedia of Polymeric Materials,* Vol. 6, J. C. Salamone, Ed., CRC Press, Boca Raton, FL, 1996, p. 4333.
5. J. O. Stoffer and T. Bone, *J. Dispersion Sci. Tech.,* **1,** 37 (1980); *J. Polym. Sci., Polym. Chem. Ed.,* **18,** 2641 (1980).
6. S. S. Atik and J. K. Thomas, *J. Am. Chem. Soc.,* **103,** 4279 (1983); *J. Am. Chem. Soc.,* **105,** 4515 (1983).
7. J. S. Guo, M. S. El-Aasser, and J. W. Vanderhoff, *J. Polym. Sci., Polym. Chem. Ed.,* **27,** 691 (1989).
8. V. H. Pérez-Luna, J. E. Puig, V. M. Castaño, B. E. Rodríguez, A. K. Murthy, and E. W. Kaler, *Langmuir,* **6,** 1040 (1990).
9. L. M. Gan, C. H. Chew, I. Lye, and T. Imae, *Polym. Bull.,* **25,** 193 (1990).
10. L. M. Gan, C. H. Chew, and I. Lye, *Makromol. Chem.,* **193,** 1249 (1992).
11. L. Feng and K. Y. Ng, *Macromolecules,* **23,** 1048 (1990); *Colloids Surf.,* **53,** 349 (1991).
12. E. Haque and S. Qutubuddin, *J. Polym. Sci., Polym. Lett. Ed.,* **26,** 429 (1988).
13. Y. S. Leong and F. Candau, *J. Phys. Chem.,* **86,** 2269 (1982).
14. F. Candau, Y. S. Leong, G. Pouyet, and S. Candau, *J. Colloid Interface Sci.,* **101,** 167 (1984).
15. F. Candau, Y. S. Leong, G. Pouyet, and R. Fitch, *J. Polym. Sci., Polym. Chem. Ed.,* **23,** 193 (1985).
16. J. Texter, L. Oppenheimer, and J. R. Minter, *Polym. Bull.,* **27,** 487 (1992).
17. A. P. Full, J. E. Puig, L. U. Gron, E. W. Kaler, J. R. Minter, T. H. Mourey, and J. Texter, *Macromolecules,* **25,** 5157 (1992).
18. J. E. Puig, V. H. Pérez-Luna, M. Pérez-González, E. R. Macías, B. E. Rodríguez, and E. W. Kaler, *Colloid Polym. Sci.,* **271,** 114 (1993).
19. L. A. Rodríguez-Guadarrama, E. Mendizábal, J. E. Puig, and E. W. Kaler, *J. Appl. Polym. Sci.,* **48,** 775 (1993).
20. L. M. Gan and C. H. Chew, *Polymer,* **34,** 3064 (1993).
21. L. M. Gan, C. H. Chew, S. C. Ng, and S. E. Loh, *Langmuir,* **9,** 2799 (1993).
22. A. P. Full, E. W. Kaler, J. Arellano, and J. E. Puig, *Macromolecules,* **29,** 2764 (1996).
23. J. Brandrup and E. H. Immergut, *Polymer Handbook,* Wiley, New York, 1989.
24. R. C. Weast, Ed., *CRC Handbook of Chemistry,* CRC Press, Boca Raton, FL, 1969.
25. R. G. Gilbert, *Emulsion Polymerization,* Academic Press, New York, 1995.
26. D. C. Blackley, *Emulsion Polymerization, Theory and Practice,* Wiley, New York and Toronto, 1975.
27. G. Odian, *Principles of Polymerization,* Wiley, New York, 1981.
28. Y. T. Choi, M. S. El-Aasser, E. D. Sudol, and J. W. Vanderhoff, *J. Polym. Sci., Polym. Chem. Ed.,* **23,** 2973 (1985).
29. *Azo Polymerization Initiator Technical Brochure,* Wako Pure Chemical Industries, Ltd., Osaka, Japan, 1987.
30. J. P. Friend and A. E. Alexander, *J. Polym. Sci., Polym. Chem. Ed.,* **6,** 1833 (1968).
31. L. A. Rodriguez-Guadarrama, M.S. Thesis, Universidad de Guadalajara, Mexico, 1993.
32. E. R. Macías, L. A. Rodríguez-Guadarrama, B. A. Cisneros, A. Castañeda, E. Mendizábal, and J. E. Puig, *Colloids Surf.,* **103,** 119 (1995).
33. P. Neta, R. E. Hule, and A. B. Ross, *J. Phys. Chem. Ref. Data,* **17,** 1027 (1988).
34. R. G. López, M. E. Treviño, M. Solís, A. Zaragoza, J. E. Puig, R. Peralta, E. Mendizábal, A. Mondragón, and V. M. Castaño, *Polytechnia (Francia),* to appear.
35. E. Mendizábal, J. Flores, J. E. Puig, F. López-Serrano, and J. Alvarez, *Eur. Polym. J.,* to appear.

Received February 20, 1996
Accepted April 29, 1996